HHS Public Access

Author manuscript

Circ Res. Author manuscript; available in PMC 2022 February 05.

Published in final edited form as:

Circ Res. 2021 February 05; 128(3): 419–432. doi:10.1161/CIRCRESAHA.120.318239.

Structural and Functional Characterization of A $Na_v1.5$-Mitochondrial Couplon

Marta Pérez-Hernández[1], **Alejandra Leo-Macias**[1], **Sarah Keegan**[2], **Mariam Jouni**[3], **Joon-Chul Kim**[1], **Esperanza Agullo-Pascual**[1], **Sarah Vermij**[1], **Mingliang Zhang**[1], **Feng-Xia Liang**[4], **Paul Burridge**[3], **David Fenyö**[2], **Eli Rothenberg**[2], **Mario Delmar**[1]

[1]Leon H Charney Division of Cardiology NYU Grossman School of Medicine. New York, NY.

[2]Institute for Systems Genetics and Department of Biochemistry and Molecular Pharmacology. NYU Grossman School of Medicine. New York, NY.

[3]Department of Pharmacology, Northwestern University Feinberg School of Medicine. Chicago, IL.

[4]Microscopy laboratory, Division of Advanced Research Technologies. NYU Grossman School of Medicine. New York, NY.

Abstract

Rationale: The cardiac sodium channel $Na_v1.5$ has a fundamental role in excitability and conduction. Previous studies have shown that sodium channels cluster together in specific cellular subdomains. Their association with intracellular organelles in defined regions of the myocytes, and the functional consequences of that association, remain to be defined.

Objective: To characterize a subcellular domain formed by sodium channel clusters in the crest region of the myocytes, and the subjacent subsarcolemmal mitochondria (SSM).

Methods and Results: Through a combination of imaging approaches including super-resolution microscopy and electron microscopy we identified, in adult cardiac myocytes, a $Na_v1.5$ subpopulation in close proximity to SSM; we further found that SSM preferentially host the mitochondrial Na^+/Ca^{2+} exchanger (NCLX). This anatomical proximity led us to investigate functional changes in mitochondria resulting from sodium channel activity. Upon TTX exposure, mitochondria near $Na_v1.5$ channels accumulated more Ca^{2+} and showed increased ROS production when compared to interfibrillar mitochondria. Finally, crosstalk between $Na_v1.5$ channels and mitochondria was analyzed at a transcriptional level. We found that *SCN5A* and *SLC8B1* (which encode $Na_v1.5$ and NCLX, respectively) are negatively correlated both in a human transcriptome dataset (GTEx) and in human-induced pluripotent stem cell-derived cardiac myocytes deficient in *SCN5A*.

Address correspondence to: Dr. Mario Delmar, The Leon H Charney Division of Cardiology, New York University School of Medicine, 435 East 30th Street. NSB 707, New York NY 10016, Tel: (212)263-9492, Mario.delmar@nyumc.org.

DISCLOSURES

None.

Conclusions: We describe an anatomical hub (a couplon) formed by sodium channel clusters and SSM. Preferential localization of NCLX to this domain allows for functional coupling where the extrusion of Ca^{2+} from the mitochondria is powered, at least in part, by the entry of sodium through $Na_v1.5$ channels. These results provide a novel entry-point into a mechanistic understanding of the intersection between electrical and structural functions of the heart.

Graphical Abstract

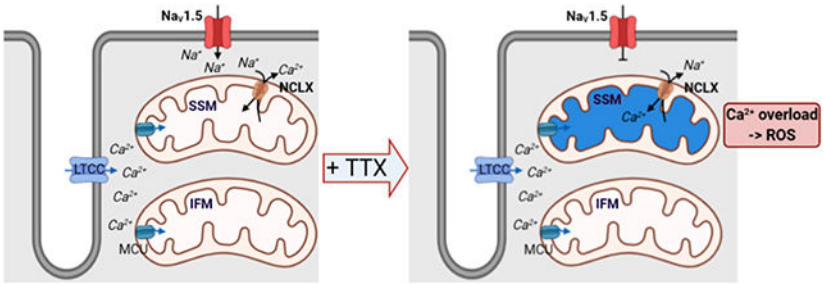

Keywords

$Na_v1.5$/ subsarcolemmal mitochondria/ NCLX/ mitochondrial homeostasis; sodium channels; mitochondria; Na+/Ca2+ exchange

Subject Terms:

Basic Science Research; Cell Biology/Structural Biology; Ion Channels/Membrane Transport; Metabolism

INTRODUCTION

The voltage-gated sodium channel (Na-channel) is central to cardiac electrogenesis. Its dysfunction can lead to lethal arrhythmias both in acquired (ischemia;[1, 2] heart failure[2]), and genetic disorders.[3-5] Rare and common genetic variants in *SCN5A*, encoding the pore-forming Na-channel subunit $Na_v1.5$, are strongly associated with life-threatening arrhythmias[4, 6] and with structural heart disease.[7-9] Yet, insight into Na-channel function, particularly as it extends beyond electrogenesis, is limited.

Na-channels form macromolecular complexes that cluster at specific subcellular domains (or "pools").[10-12] An emerging concept is that certain Na-channel partners localize only to one subcellular domain, thus endowing the functional complex with region-specific properties that, if disrupted, facilitate arrhythmias.[13-17]

Subcellular organelles such as mitochondria also organize in region-specific subdomains. Mitochondria in myocytes are highly organized, spatially separated into at least three subpopulations: one just beneath the surface sarcolemma (subsarcolemmal mitochondria, SSM), a second one (the largest fraction) between myofibrils in longitudinal chains (interfibrillar mitochondria, IFM), and a third one, occupying the perinuclear subdomain (PNM). Data show that these subpopulations possess distinct biochemical properties,

morphology, Ca^{2+} handling, and that they may interact differently with other intracellular structures, causing functional specificity.[18,19]

The relationship between Na-channel and mitochondrial function is well established in one direction only: mitochondrial function and/or molecular composition can alter sodium current (I_{Na}).[20,21] Recently, however, Zhang *et al* demonstrated that reduced levels of *Scn5a* expression lead to accumulation of myocardial reactive oxygen species (ROS),[22] and Wan *et al* documented that expression of $Na_v1.5$ mutant F1759A leads to mitochondrial injury.[23] The mechanism by which sodium channel expression or activity can affect mitochondrial function or integrity is not known.

We investigated the anatomical and functional relation between mitochondria and $Na_v1.5$ in adult cardiac myocytes. Advanced imaging methods allowed us to observe that a subpopulation of membrane-resident $Na_v1.5$ clusters sits in close apposition to subjacent SSM, and that it is in this mitochondrial subpopulation where the mitochondrial Na^+/Ca^{2+} exchanger (NCLX; encoded by *SLC8B1*) is primarily located. This anatomical proximity led us to investigate functional changes in mitochondria resulting from Na-channel activity. In particular, exposing adult cardiac myocytes to the Na-channel blocker tetrodotoxin (TTX) caused accumulation of mitochondrial Ca^{2+} and ROS production, predominantly in SSM. We speculate that proximity to functional $Na_v1.5$ clusters facilitates sodium-dependent activity of NCLX to extrude mitochondrial Ca^{2+}, whereas reduced sodium entry impairs Ca^{2+} extrusion. In addition, we observed that the relation between $Na_v1.5$ and NCLX is not only local. Indeed, human transcriptome analysis shows that *SCN5A* negatively correlates with *SLC8B1*. Experimental confirmation was obtained from human-induced pluripotent stem cell-derived cardiomyocytes (hiPSC-CM) in which *SCN5A* was knocked down. We conclude that not only mitochondrial metabolism can affect I_{Na} but Na-channels can, in turn, positively affect mitochondrial function. Our data lead us to propose the existence of a Na-channel subpopulation that clusters with subjacent mitochondria to create an anatomical couplon for electro-metabolic coupling.

METHODS

Data Availability.

The authors declare that all supporting data are available within the article and its Online supplement files.

Expanded Methods available in Online Data Supplement.

Mice.

Wild-type black mice C57BL/6N strain 027 (Charles River Laboratories) were treated in accordance to the Guide for Care and Use of Laboratory Animals published by the US National Institutes of Health. Procedures were approved by the NYU IACUC committee, protocol 160726. Both genders were included and animals were between 3-6 months of age.

Focused Ion Beam-Scanning Electron Microscopy (FIB-SEM).

Protocol modified from Wilke *et al.* [24] Tissue was processed and e*n bloc* lead staining performed to enhance membrane contrast.[25] Acquisition was done using Auto Slice and View G3 software.[26]

Inmunostaining.

For immunolocalization, HL-1 cells were incubated with Mitotracker and NCLX antibody, as described in Online Supplement Data.

Cardiomyocyte dissociation.

Adult mouse ventricular myocytes were obtained by enzymatic dissociation, as described in Online Supplement Data.

Single-molecule localization microscopy (SMLM) by stochastic optical reconstruction microscopy (STORM).

Ventricular cardiomyocytes were incubated with Mitotracker before fixation and immunostained with NCLX, $Na_v1.5$ and α-actinin antibodies. Interaction factor analysis (details in Supplemental Data) provided a measure of the degree to which mitochondria and $Na_v1.5$ proximity can be the result of random (*vs* deterministic) distribution.

Mitochondrial Ca^{2+} dynamics.

As described,[27] mitochondrial Ca^{2+} was measured with Rhod-2-AM dye. Analysis and quantification were done using LASX and ImageJ software. To evaluate mitochondrial Ca^{2+} dynamics in response to drugs, we monitored Rhod-2 fluorescence signal before (F_0) and after (F) adding: TTX, carbonyl cyanide 4-(trifluoromethoxy) phenylhydrazone (FCCP) + oligomycin A and CGP-37157.

Mitochondrial superoxide detection.

Superoxide production was measured using MitoSOX, per manufacturer's instructions. To evaluate mitochondrial superoxide changes in response to TTX, we measured MitoSOX fluorescence signal before (F_0) and after (F) TTX.

SCN5A correlation analysis in human left ventricle.

RNAseq raw data from human left ventricular tissue were downloaded from the Genotype-Tissue Expression v8 (GTEx) consortium (https://www.gtexportal.org/home/datasets). Analysis done using Rstudio.

hiPSC-CM model of SCN5A knockout.

hiPSCs were maintained as previously described.[28] CRISPR/Cas9 was used to generate the *SCN5A* knock-out line. Differentiation into hiPSC-CMs was modified from a previously described protocol.[29,30]

Statistics.

Numerical results are given as means±standard error of the mean (S.E.M.). Statistical tests were used as stated. Differences were considered significant at $p<0.05$.

RESULTS

Mitochondria are in close apposition to the sarcolemma.

Figure 1A shows an electron microscopy image of mouse left ventricle revealing the alignment of mitochondria along the interfibrillar space. A complete volumetric image of cardiac tissue acquired using FIB-SEM (Fig. 1B) showed mitochondria "nested" immediately under the sarcolemma in the dome-shaped surface spanning the distance between z-disks (the "crest"[31]), with both structures (sarcolemma and SSM) reaching points of close apposition (red arrows; small panels show different planes of the same preparation). A zoom-in of Figure 1B-A, with detailed description of structures observed in the left end of the image, is presented in Supplemental Fig.I. Segmentation analysis of FIB-SEM images facilitated visualization (Fig. 1C) and revealed multiple connections of SSM with deeper mitochondria both immediately subjacent and, through mitochondria that bridge across sarcomeres, to other interfibrillar chains in the cell, hence expanding into a complete mitochondrial reticulum[31] (Fig. 1C and Supplemental Fig.II). Approximately 13% of the mitochondrial surface in the subsarcolemmal space was found <20 nm apart from the membrane (Supplemental Fig.III).

$Na_v1.5$ clusters adjacent to SSM in a non-random organization.

In separate experiments, we used dual-color STORM to localize $Na_v1.5$ in the membrane surface of adult ventricular myocytes. α-Actinin was used to mark sarcomeric edges (z-disks). As shown in Figure 2A, we observed large $Na_v1.5$ clusters between z-disks, in agreement with previous functional data.[14] Negative controls are shown in Supplemental Fig.IV. $Na_v1.5$ distribution led us to speculate that a subpopulation of Na-channels may localize in close proximity to SSM, creating a macromolecular complex.

Figure 2B presents an image of a single, isolated adult cardiac myocyte labeled for $Na_v1.5$ (green) and Mitotracker (red) to localize mitochondria. At the cell lateral membrane (distinguishable as the edge framing the long axis of the cell) a seemingly preferential proximity of mitochondria and $Na_v1.5$ was noted (white rectangles indicating area enlarged in the bottom of each panel). For some experiments, a third color was added (blue) to mark α-actinin (Fig. 2C). Data are consistent with the localization of $Na_v1.5$ and of mitochondria separately detected by FIB-SEM and by STORM (Figs. 1 and 2A, respectively). Moreover, the organization of both resembles the shape of the crest, with a $Na_v1.5$ cluster resting on top of the mitochondria, and between z-disks. $Na_v1.5$ cluster properties are indicated in Supplemental Fig.V.

We developed an analytical tool to address the question of whether proximity is random or deterministic. A line traced over the aligned SSM was used as reference (Fig. 3A). Each $Na_v1.5$ cluster was defined as an ellipse. Two parameters were defined: the distance between the centroid of the ellipse and the reference line, and the angle formed between the long axis

of the ellipse, and the reference line (details on online supplement). Parameters were correlated for each cluster on an xy plot (Fig. 3B). Experimental data were compared to a simulated image where mitochondria were kept as in the experimental data but $Na_v1.5$ clusters were distributed randomly, though constrained by the edge of the cell (Fig. 3C-D). As shown in Figure 3B, most experimental $Na_v1.5$ clusters assembled in a small window of 10 to 300 nm in distance and a 0-60° angle to the reference line. However, in simulated images, green clusters were scattered along the plot (Fig. 3D). The method was further validated when comparing the relation between SSM and a line formed by immunostaining of α-actinin, which traces the z-disk perpendicular to the lateral surface of the membrane. In this case, almost all α-actinin clusters were gathered in a very small window, with a 500 to 2000 nm distance and a 70-90° angle to the mitochondria long axis, as expected (Fig. 3E-H). Overall, our results support the concept that the Na-channel complex and mitochondria form a structural macromolecular complex. Whether the association has a functional correlate was investigated next.

Mitochondrial NCLX is predominantly found in SSM near $Na_v1.5$ clusters.

NCLX plays an important role in maintaining mitochondrial function. Sodium concentration, in turn, is key to the ability of NCLX to extrude Ca^{2+} from the mitochondrial space. Given the found relation between $Na_v1.5$ and mitochondria, we examined whether NCLX had a preferential localization in the SSM space.

Figure 4 shows that the immunofluorescent signal for NCLX (red) was more abundant in the SSM than in mitochondria localized in the intracellular space; we also show significant co-localization of NCLX with $Na_v1.5$-positive clusters (green). Indeed, ~80% of $Na_v1.5$-NCLX clusters colocalized (i.e., were located within 20 nm of each other) at the lateral membrane *vs* ≈30% in the cell interior (Supplemental Fig. VI). To further validate NCLX antibody specificity for mitochondrial NCLX, we immunolocalized mitochondria with NCLX in HL-1 cells. Supplemental Fig.VII shows colocalization of the two structures and a round-punctuate pattern, characteristic of mitochondrial structures.

Given the proximity of NCLX to $Na_v1.5$, we postulated that the presence or absence of I_{Na} may impact on NCLX function and as such, on the extent of Ca^{2+} accumulation in the mitochondrial space.

Mitochondrial Ca^{2+} dynamics: differences between SSM and IFM.

To assess the relation between NCLX and Na-channel function we used a mitochondrial Ca^{2+} indicator (Rhod2-AM; Fig. 5A; see also Supplemental Fig.VIII.A, “Methods” and[27]). Supplemental Fig.IX shows preservation of striated cell morphology after treatment. Rhod2-AM intensity was measured before (F_0) and after drug treatment (F) and measurements of the ratio F/F_0 in SSM were compared to those obtained in IFM. Measurements in control conditions (no drugs added) are shown as the first two bars of the graph in Figure 5B, corresponding to data acquired from SSM (red) and IFM (gray), respectively. Since cytoplasmic Na^+ concentration is a major driver of NCLX forward movement, we first tested whether blocking I_{Na} with TTX would affect mitochondrial Ca^{2+}. Rhod2-AM fluorescence was first recorded in a solution containing 148 mmol/L Na^+; then, TTX 10 μmol/L was

added. The bar graph (bars with vertical lines) in Figure 5B shows that, upon TTX exposure, SSM accumulated significantly more Ca^{2+} (detected as increase in Rhod2 fluorescence) than IFM (F/F_0 1.1±0.03 and 0.99±0.03 for SSM and IFM, respectively; $p<0.05$). This was consistent with the notion that reduced entry of sodium via $Na_v1.5$ limits NCLX activity, and that this effect is more noticeable in the area where the $Na_v1.5$/NCLX complex is abundant (see Supplemental Fig.VIII.B). Of note, when low concentrations of TTX (100 nmol/L) were used, we observed a non-statistically significant tendency for increased Rhod2 intensity in SSM (Supplemental Fig.X).

We next compared Ca^{2+} dynamics in SSM *vs* IFM in the presence of TTX and after mitochondrial depolarization with 1 μmol/L FCCP + 2 μmol/L oligomycin. FCCP alone can induce mitochondrial ATP depletion via the reverse of F_0/F_1-ATPase, which is prevented by adding the F_0/F_1-ATPase inhibitor oligomycin. FCCP induces a mitochondrial depolarization of around 100 mV, enough for NCLX to function in reverse mode (Ca^{2+}_{in}/ Na^{+}_{out} of the mitochondria).[32] Consistent with this notion, FCCP+oligomycin augmented Rhod2 fluorescence exclusively at the SSM (Fig. 5B, bars with horizontal lines). Most importantly, adding the NCLX inhibitor CGP-371257 attenuated the mitochondrial Ca^{2+} accumulation in SSM and no significant difference in Rhod2 fluorescence was observed between SSM and IFM (Fig. 5B, bar with dots).

We analyzed Rhod2 fluorescence in cells treated only with 2 μmol/L CGP-37157, a selective NCLX inhibitor. As expected, after adding CGP-37157, Rhod2 fluorescence increased in SSM (ratio 1.10±0.024 *vs* IFM ratio 0.98±0.01, $p<0.001$, Fig. 5B bars with crosses) indicating that Ca^{2+} influx through the mitochondrial calcium uniporter (MCU) cannot be compensated by extrusion since NCLX is inhibited. Rhod2 fluorescence was practically unchanged after CGP-37157 addition in IFM, suggesting that IFM have another way of extruding Ca^{2+} that is NCLX- and Na^{+}-independent.

Finally, we measured mitochondrial Ca^{2+} dynamics at different pacing rates (3 and 5Hz) alone or in the presence of either TTX or CGP-37157. Rapid pacing led to mitochondrial Ca^{2+} accumulation in SSM and IFM (vs rest #$p<0.05$). When TTX was added (10 μmol/L), there was a tendency for SSM to accumulate more Ca^{2+} in response to pacing (3Hz vs 3Hz+ TTX $p=0.06$; 5Hz vs 5Hz+ TTX $p=0.07$) and when comparing the two mitochondrial subpopulations, mitochondrial Ca^{2+} increased significantly more in SSM than in IFM, *$p<0.05$). Similar results were obtained with CGP-37157. Details in Supplemental Fig.XI. Altogether, the data suggest functional coupling between $Na_v1.5$ and NCLX in the sarcolemmal-subsarcolemmal space in the crest region of adult cardiac myocytes, with functional implications to the adaptation necessary to meet demand at increased rates.

Increased superoxide production after TTX addition.

There is a reciprocal interaction between Ca^{2+} and ROS which, in physiological conditions, plays an important role in regulating cellular signaling networks.[33,34] Pathological changes in one can affect the other, leading to more damage. Since TTX increases mitochondrial Ca^{2+}, we wondered if this could lead to increased ROS production.

We used the fluorescent dye MitoSOX Red, which detects mitochondrial superoxide, to measure ROS in live myocytes before and after TTX. When in mitochondria, MitoSOX exhibits red fluorescence. As seen in Figure 6, at resting conditions (F_0) ventricular myocytes showed low MitoSOX fluorescence, higher in SSM, as previously reported.[35] Co-staining with MitoTracker confirmed MitoSox mitochondrial localization (Supplemental Fig.XII).

After exposure to TTX 10 μmol/L (pacing at 0.5Hz), MitoSOX fluorescence increased in both SSM and IFM, the latter being less pronounced (Paired Student's t-test: $p<0.001$ +TTX vs rest in SSM; $p<0.05$ +TTX vs rest in IFM). This result indicates that blocking Na^+ entry with TTX leads to increased mitochondrial ROS production, though in this case there was no predominant effect in the SSM, suggesting that the role of I_{Na} on mitochondrial function may go beyond its local interaction with NCLX.

Correlation analysis of human left ventricle transcriptome in relation to SCN5A expression.

We used the Genotype-Tissue Expression repository (GTEx; v8) of 386 samples of left ventricle tissue from deceased human donors to compare the abundance of *SCN5A* transcript against *SLC8B1* and *SLC8A1*, which encode the mitochondrial NCLX and the plasma membrane NCX, respectively. Resulting plots are shown in Figure 7A-B. Data show that *SLC8A1* is positively correlated with *SCN5A* (regression coefficient β= 0.62, log-*P*-value= 4E-58) whereas *SLC8B1* is negatively correlated with *SCN5A* (regression coefficient β= −0.17, log-*P*-value= 1.66 E-30). This observation is only correlational. We therefore tested whether reduced abundance of one transcript would affect the abundance of the other. To this aim, we used an hiPSC-CM line deficient in *SCN5A* (see "Methods" and Supplemental Figs.XIII and XIV). As shown in Figure 7C the abundance of *SLC8B1* was significantly increased in cells where *SCN5A* was knocked down, supporting the notion of a transcriptional relation between the two gene products.

DISCUSSION

Our data show that SSM and a subpopulation of $Na_v1.5$ at the lateral membrane are in close apposition and that in ventricular cardiomyocytes, not only mitochondria can regulate I_{Na},[20,21] but also I_{Na} can regulate NCLX activity. NCLX preferentially localized at SSM near $Na_v1.5$ clusters. We speculate that such distribution creates a high-Na^+ microdomain that is energy-efficient, comparable to the high-Ca^{2+} microdomain formed between MCU and the sarcoplasmic reticulum (SR). Many diseases have been linked to changes in intracellular Na^+ concentration[36] which, in turn, could affect NCLX function, therefore affecting ATP production and ROS generation. Overall, we show the presence of a Na-channel-mitochondria complex and suggest that $Na_v1.5$-NCLX proximity may have functional consequences to metabolic homeostasis via crosstalk with the mitochondrial reticulum.

Cardiomyocytes are rich in mitochondria, which occupy a third of total cell volume.[18] Although mitochondria form a network reaching throughout the cell[37,38], they are divided into at least three subpopulations with distinct morphology, composition, biochemical properties and function, contributing to their capacity for adaptation.[18,19,35] Here, we focus on SSM. As others,[39] we found SSM nested in-between z-disks. A nanometric-resolution

cell-surface scan shows a pattern of crests and valleys (or “grooves”) with ~2 μm periodicity, that is, the length of a sarcomere.[31] In this pattern, grooves match the position of the z-disk (prompting the name “z-grooves”), with crests being dome-shaped surfaces spanning the distance between two z-grooves.[31] Previously, using scanning patch clamp, we measured larger I_{Na} in the crest compared to grooves.[14] This matches our data showing $Na_v1.5$ clusters preferentially aligned with SSM at the crest. We also show that the cell membrane in the crest region reaches close proximity with the outer membrane of the mitochondria, in a manner reminiscent of the T-tubule-junctional SR dyad (see, e.g.[40,41]) or between cell membranes in the perinexus.[42] In these structures, the narrow intermembrane space allows functional coupling between channels residing in opposing membranes. The molecular mechanisms of formation of this $Na_v1.5$-mitochondrial complex remain undefined. Yet, we show that the relation between mitochondria and $Na_v1.5$ is deterministic and of a particular topology.

We identify NCLX, a molecule key for Na^+ and Ca^{2+} homeostasis, as resident of the $Na_v1.5$-mitochondria hub. NCLX (encoded by *SLC8B1*) is proposed to be the main pathway for mitochondrial Ca^{2+} extrusion in excitable cells, while MCU is responsible for Ca^{2+} transport into mitochondria.[43,44] NCLX transport is voltage-dependent and electrogenic, with stoichiometry of 3-4 Na^+ for 1 Ca^{2+}.[45] Unlike plasma membrane NCX, unique residues confer NCLX Li^+ selectivity.[46] The Ca^{2+} extrusion rate of NCLX is ≈100 times slower than MCU-Ca^{2+} influx rate. Therefore, NCLX activity is the rate-limiting step of mitochondrial Ca^{2+} cycling.[44,47,48]

NCLX is fundamental to life. A conditional knockout of NCLX quickly leads to heart failure associated with mitochondrial Ca^{2+} overload and consequent increase in ROS generation.[43] In contrast, NCLX overexpression in mouse heart increases mitochondrial Ca^{2+} extrusion preventing pathogenic Ca^{2+} accumulation and ROS generation.[43] Whether loss or over-abundance of NCLX affects I_{Na} or subcellular localization of $Na_v1.5$ remains unclear.

NCLX is very sensitive to changes in cytoplasmic [Na^+],[32,48,49] given that the Km of association is similar to resting $[Na^+]_i$ (K_m ~7-10 mmol/L). Moreover, studies from Skogestad et al show that $[Na^+]_i$ in an active, excitable myocyte, is not homogeneous. Rather, it is highest in the subsarcolemma and distributes in pools, likely, corresponding to the location of Na^+-channel clusters.[50] We propose that NCLX is close to $Na_v1.5$ channels to rapidly sense Na^+ signals and properly extrude Ca^{2+} out of mitochondria, in a way similar to how MCU’s low affinity for Ca^{2+} is compensated by proximity to the SR (diagram in Supplemental Fig.VIII).[51,52] Several studies describe an interaction of NCLX with plasma membrane transporters: a) In pancreatic β-cells, glucose-dependent depolarization leads to cytosolic Na^+ influx via voltage-gated Na^+ channels, which promotes NCLX activity, maintaining ATP production and controlling insulin secretion.[53,54] b) The nociceptive noxious heat-activated receptor (TRPV1) triggers a Na^+-dependent depolarization that controls NCLX Ca^{2+} extrusion, which at the same time regulates TRPV1 conductance.[55,56] c) In macrophages and melanoma cells, activation of a splice variant of $Na_v1.6$ causes release of Na^+ from vesicular compartments and Na^+-uptake-Ca^{2+}release by NCLX.[57]

Through human transcriptome analysis, we found *SLC8B1* negatively correlating with *SCN5A*. Though the common denominator of this relation remains unknown, its presence may have important functional consequences. Indeed, reduced expression of *SCN5A* may be compensated by increased expression of *SCL8B1* to increase the ability to capture Na^+ entering the cell. The reverse would also have functional effects: an excess Na^+ entry could be compensated by reduced expression of the exchanger, maintaining mitochondrial homeostasis. This is consistent with the notion that NCLX activity is strongly regulated by even slight changes in cytosolic Na^+.[48,58-63] Their physical proximity (shown here) and transcriptional inverse relation would facilitate maintenance of this delicate equilibrium.

In resting Na^+ and Ca^{2+} conditions and with an inner mitochondrial membrane potential of ~ −180 mV, NCLX operates in forward mode, exporting Ca^{2+} out of the mitochondrial matrix in exchange for cytosolic Na^+. However, in depolarized mitochondria, NCLX functions in reverse mode, transporting Ca^{2+} into the mitochondria and extruding Na^+.[64] Studies have shown that increasing cytosolic Na^+ accelerates mitochondrial Ca^{2+} decay due to increased NCLX forward mode activity,[63,64] but these studies did not compare SSM to IFM. Our mitochondrial Ca^{2+} dynamic experiments show that NCLX is predominantly located at SSM, confirming our SMLM experiments, and TTX leads to mitochondrial Ca^{2+} accumulation more prominently in SSM, connecting $Na_V1.5$ and NCLX function. The Ca^{2+} accumulation after TTX+FCCP+Oligomycin exposure in SSM seen in our experiments could be explained by 1) active uptake of calcium by the reverse NCLX, or 2) increased mitochondrial uptake via MCU. However, MCU open probability decreases with mitochondrial depolarization (i.e. with FCCP).[64] In fact, IFM show a slight decrease in Rhod2 fluorescence after TTX+FCCP+Oligomycin which could be accounted for an inhibited MCU and lack of reverse mode NCLX-Ca^{2+} uptake in IFM. We used the benzothiazepine compound CGP-37157 to selectively block NCLX (IC_{50}= 0.36 μM).[59,62] At least a 10-fold higher concentration of CGP-37157 is needed to affect plasma membrane NCX, SERCA and RyR2.[59] It is known that cytosolic Na^+ is required for powering NCLX to activate mitochondrial Ca^{2+} efflux. Therefore, our mitochondrial Ca^{2+} dynamics data suggest that a healthy I_{Na} is needed to maintain mitochondrial Ca^{2+} homeostasis. However, and compared to Ca^{2+} imaging, studying cellular Na^+ dynamics is challenging, particularly due to the relatively small changes of intracellular Na^+ concentration.[53,58]

There is mutual interaction between ROS and Ca^{2+}, where ROS can regulate Ca^{2+} signaling and Ca^{2+} signaling is essential for ROS production.[33,43] Physiologically, ROS are generated as by-product of mitochondrial respiratory chain activity or by specialized ROS-generating enzymes to regulate signaling functions such as cell proliferation, migration, and vascular tone; but toxic levels associate with pathology. Mitochondrial Ca^{2+} accumulation leads to ROS production. Our results show increased ROS production after TTX exposure in both SSM and (less pronounced) IFM, even though only SSM showed increased mitochondrial Ca^{2+} after TTX. It is worth noting that, even though they are part of distinct mitochondrial subpopulations, SSM and IFM are connected, forming a mitochondrial reticulum in which ROS can propagate.[37,38,65] Most importantly, ROS production leads to decreased I_{Na}.[66] ROS can alter the oxidative state of PKA, PKC, CaMKII and NAD(H), which in turn regulates I_{Na}.[33,67] Genetically engineered *Scn5a* heterozygous mice show increased ROS accumulation.[68] This, together with our results, suggests that there could be an amplification

loop: increased ROS decreases I_{Na}, leading to less Na^+ entering the cytoplasm, which in turn affects NLCX activity which leads to mitochondrial Ca^{2+} accumulation, leading to more ROS production.

One question that arises is how do IFM extrude calcium if NCLX is mainly found in SSM? Even though NCLX is the major transporter for Ca^{2+} extrusion, mitochondria contain both Na^+-dependent and Na^+-independent mechanisms for Ca^{2+} extrusion.[45,64] This may include leucine zipper EF-hand-containing transmembrane protein 1 (LETM1;[45,64,69]). Somehow controversial, it has been proposed that transient mitochondrial permeability transition pore openings could also help discharge mitochondrial Ca^{2+} load.[45,47,70] Other studies show Cx43 hemichannels in mitochondria[71] and particularly in SSM[72] which could act as mitochondrial Ca^{2+} gateway. Overall, our data are consistent with previous descriptions of proteins that distribute and/or work differently in various sub-populations of mitochondria (see, e.g.[73,74]).

Our data suggest the need of healthy I_{Na} for (proper) mitochondrial Ca^{2+} balance. Many diseases associate with cytoplasmic unbalanced Na^+ concentration. A pathogenic increase in cytoplasmic Na^+ accelerates mitochondrial Ca^{2+} efflux trough NCLX, which inhibits mitochondrial metabolic rate and ATP production, as seen in heart failure, ischemia, and seizure-like events.[48,59,63,75,76] In melanoma cells, an increase in Na^+ mediated by vesicular $Na_v1.6$ activates NCLX, which accelerates invasiveness of these tumor cells.[57] Conversely, hypoxia is known to reverse NCLX mode, which leads to mitochondrial Ca^{2+} overload and ROS production, in turn accelerating cytoplasmic Na^+ accumulation.[77] Future studies need to be done to analyze NCLX activity in pathologies where I_{Na} is reduced (e.g. Brugada syndrome).

Supplementary Material

Refer to Web version on PubMed Central for supplementary material.

ACKNOWLEDGMENTS

We thank Chris Petzold for EM sample preparation and image acquisition. GTEx Project was supported by the Common Fund of the Office of the Director of the National Institutes of Health, and by NCI, NHGRI, NHLBI, NIDA, NIMH, and NINDS.

SOURCES OF FUNDING

Supported by NIH RO1-HL134328, RO1-HL136179 and RO1-HL145911 (MD), the Wilton W. Webster Fellowship in Pediatric Electrophysiology from the Heart Rhythm Society (MP-H), a Leducq Foundation Transatlantic network of Excellence (MD, PB) and the Swiss National Science Foundation P1BEP3_172237 (SV). Microscopy Laboratory is supported by: NIH/NCI P30CA016087 and S10 ODO019974-01A1.

Nonstandard Abbreviations and Acronyms:

FIB-SEM	Focused Ion Beam-Scanning Electron Microscopy
GTEx	Genotype-Tissue Expression
IFM	InterFibrillar Mitochondria

SSM	SubSarcolemmal Mitochondria
NCLX	Mitochondrial $Na^+/Ca^{2+}/Li^+$ Exchanger
ROS	Reactive Oxygen Species
SMLM	Single-Molecule Localization Microscopy
STORM	Stochastic Optical Reconstruction Microscopy
TTX	Tetrodotoxin

REFERENCES

1. Janse MJ and Wit AL. Electrophysiological mechanisms of ventricular arrhythmias resulting from myocardial ischemia and infarction. Physiological reviews. 1989;69:1049–169. [PubMed: 2678165]
2. Bankston JR and Kass RS. Fading sodium channels in failing hearts. Circ Res. 2007;101:1073–4. [PubMed: 18040022]
3. Wilde AA and Brugada R. Phenotypical manifestations of mutations in the genes encoding subunits of the cardiac sodium channel. Circ Res. 2011;108:884–97. [PubMed: 21454796]
4. Wilde AA, Moss AJ, Kaufman ES, Shimizu W, Peterson DR, Benhorin J, Lopes C, Towbin JA, Spazzolini C, Crotti L, Zareba W, Goldenberg I, Kanters JK, Robinson JL, Qi M, Hofman N, Tester DJ, Bezzina C, Alders M, Aiba T, Kamakura S, Miyamoto Y, Andrews ML, McNitt S, Polonsky B, Schwartz PJ, Ackerman MJ. Clinical Aspects of Type 3 Long QT Syndrome: An International Multicenter Study. Circulation. 2016;134(12):872–82. [PubMed: 27566755]
5. George AL. Inherited disorders of voltage-gated sodium channels. J Clin Invest. 2005;115:1990–9. [PubMed: 16075039]
6. Bezzina CR, Lahrouchi N, Priori SG. Genetics of sudden cardiac death. Circ Res. 2015;116:1919–36. [PubMed: 26044248]
7. te Riele AA-PE, James CA, Leo-Macias A, Cerrone M, Zhang M, Lin X, Lin B, Sobreira NL, Amat-Alarcon N, Narsman RF, Murray B, Tichnell C, can der Heijden JF, Dooijes D, van Veen TA, Tandri H, Fowleer SJ, Hauer RN, Tomaselli G, van den Berg MP, Taylor Mr, Brun F, Sinagra G, Wilde AA, Mestroni L, Bezzina CR, Calkins H, van Tintelen PJ, Bu L, Delmar M, Judge DP. Multilevel analyses of SCN5A mutations in ARVD/C suggest noncanonical mechanisms of disease pathogenesis. Cardiovasc Res. 2017;113:102–111. [PubMed: 28069705]
8. Liu M, Yang KC, Dudley SC Jr. Cardiac sodium channel mutations: why so many phenotypes? Nature reviews Cardiology. 2014;11:607–15. [PubMed: 24958080]
9. Liu M, Yang KC, Dudley SC Jr. Cardiac Sodium Channel Mutations: Why so Many Phenotypes? Curr Top Membr. 2016;78:513–59. [PubMed: 27586294]
10. Abriel H, Rougier JS, Jalife J. Ion channel macromolecular complexes in cardiomyocytes: roles in sudden cardiac death. Circ Res. 2015;116:1971–88. [PubMed: 26044251]
11. Petitprez S, Zmoos AF, Ogrodnik J, Balse E, Raad N, El-Haou S, Albesa M, Bittihn P, Luther S, Lehnart SE, Hatem SN, Coulombe A, Abriel H. SAP97 and dystrophin macromolecular complexes determine two pools of cardiac sodium channels $Na_v1.5$ in cardiomyocytes. Circ Res. 2011;108:294–304. [PubMed: 21164104]
12. Shy D, Gillet L, Abriel H. Cardiac sodium channel NaV1.5 distribution in myocytes via interacting proteins: the multiple pool model. Biochim Biophys Acta. 2013;1833:886–94. [PubMed: 23123192]
13. Lin X, Liu N, Lu J, Zhang J, Anumonwo JM, Isom LL, Fishman GI, Delmar M. Subcellular heterogeneity of sodium current properties in adult cardiac ventricular myocytes. Heart Rhythm. 2011;8:1923–30. [PubMed: 21767519]
14. Bhargava A, Lin X, Novak P, Mehta K, Korchev Y, Delmar M, Gorelik J. Super-resolution scanning patch clamp reveals clustering of functional ion channels in adult ventricular myocyte. Circ Res. 2013;112:1112–20. [PubMed: 23438901]

15. Marsman RF, Bezzina CR, Freiberg F, Verkerk AO, Adriaens ME, Podliesna S, Chen C, Purfurst B, Spallek B, Koopmann TT, Baczko I, Dos Remedios CG, George AL Jr, Bishopric NH, Lodder EM, de Bakker JM, Fischer R, Coronel R, Wilde AA, Gotthardt M, Remme CA. Coxsackie and adenovirus receptor is a modifier of cardiac conduction and arrhythmia vulnerability in the setting of myocardial ischemia. J Am Coll Cardiol. 2014;63:549–59. [PubMed: 24291282]

16. Gillet L, Rougier JS, Shy D, Sonntag S, Mougenot N, Essers M, Shmerling D, Balse E, Hatem SN, Abriel H. Cardiac-specific ablation of synapse-associated protein SAP97 in mice decreases potassium currents but not sodium current. Heart Rhythm. 2015;12(1):181–92. [PubMed: 25447080]

17. Sato PY, Coombs W, Lin X, Nekrasova O, Green KJ, Isom LL, Taffet SM, Delmar M. Interactions between ankyrin-G, Plakophilin-2, and Connexin43 at the cardiac intercalated disc. Circ Res. 2011;109:193–201 [PubMed: 21617128]

18. Piquereau J, Caffin F, Novotova M, Lemaire C, Veksler V, Garnier A, Ventura-Clapier R, Joubert F. Mitochondrial dynamics in the adult cardiomyocytes: which roles for a highly specialized cell? Front Physiol. 2013;4:102. [PubMed: 23675354]

19. Lu X, Thai PN, Lu S, Pu J, Bers DM. Intrafibrillar and perinuclear mitochondrial heterogeneity in adult cardiac myocytes. J Mol Cell Cardiol. 2019;136:72–84. [PubMed: 31491377]

20. Liu M, Sanyal S, Gao G, Gurung IS, Zhu X, Gaconnet G, Kerchner LJ, Shang LL, Huang CL, Grace A, London B, Dudley SC Jr. Cardiac Na^+ current regulation by pyridine nucleotides. Circ Res. 2009;105:737–45. [PubMed: 19745168]

21. London B, Michalec M, Mehdi H, Zhu X, Kerchner L, Sanyal S, Viswanathan PC, Pfahnl AE, Shang LL, Madhusudanan M, Baty CJ, Lagana S, Aleong R, Gutmann R, Ackerman MJ, McNamara DM, Weiss R, Dudley SC Jr. Mutation in glycerol-3-phosphate dehydrogenase 1 like gene (GPD1-L) decreases cardiac Na+ current and causes inherited arrhythmias. Circulation. 2007;116:2260–8. [PubMed: 17967977]

22. Zhang X, Yoon JY, Morley M, McLendon JM, Mapuskar KA, Gutmann R, Mehdi H, Bloom HL, Dudley SC, Ellinor PT, Shalaby AA, Weiss R, Tang WHW, Moravec CS, Singh M, Taylor AL, Yancy CW, Feldman AM, McNamara DM, Irani K, Spitz DR, Breheny P, Margulies KB, London B, Boudreau RL. A common variant alters SCN5A-miR-24 interaction and associates with heart failure mortality. J Clin Invest. 2018;128:1154–1163. [PubMed: 29457789]

23. Wan E, Abrams J, Weinberg RL, Katchman AN, Bayne J, Zakharov SI, Yang L, Morrow JP, Garan H, Marx SO. Aberrant sodium influx causes cardiomyopathy and atrial fibrillation in mice. J Clin Invest. 2016;126:112–22. [PubMed: 26595809]

24. Wilke SA, Antonios JK, Bushong EA, Badkoobehi A, Malek E, Hwang M, Terada M, Ellisman MH, Ghosh A. Deconstructing complexity: serial block-face electron microscopic analysis of the hippocampal mossy fiber synapse. J Neurosci 2013;33,507–522. [PubMed: 23303931]

25. Walton J Lead asparate, an en bloc contrast stain particularly useful for ultrastructural enzymology. J Histochem Cytochem 1979; 27, 1337–1342. [PubMed: 512319]

26. Leo-Macias A, Agullo-Pascual E, Sanchez-Alonso JL, Keegan S, Lin X, Arcos T, Feng-Xia-Liang, Korchev YE, Gorelik J, Fenyö D, Rothenberg E, Rothenberg E, Delmar M. Nanoscale visualization of functional adhesion/excitability nodes at the intercalated disc. Nat Commun 2016;7:10342. [PubMed: 26787348]

27. Kim JC, Pérez-Hernández M, Alvarado FJ, Maurya SR, Montnach J, Yin Y, Zhang M, Lin X, Vasquez C, Heguy A, Liang FX, Woo SH, Morley GE, Rothenberg E, Lundby A, Valdivia HH, Cerrone M, Delmar M. Disruption of Ca^{2+}i Homeostasis and Connexin 43 Hemichannel Function in the Right Ventricle Precedes Overt Arrhythmogenic Cardiomyopathy in Plakophilin-2-Deficient Mice. Circulation 2019;140(12):1015–1030. [PubMed: 31315456]

28. Kuo H-H, Gao X, DeKeyser J-M, Fetterman KA, Pinheiro EA, Weddle CJ, Fonoudi H, Orman MV, Romero-Tejeda M, Jouni M, Blancard M, Magdy T, Epting CL, George AL, Burridge PW. Negligible-Cost and Weekend-Free Chemically Defined Human iPSC Culture. Stem Cell Reports. 2020;14(2):256–270. [PubMed: 31928950]

29. Burridge PW, Holmström A, Wu JC. Chemically Defined Culture and Cardiomyocyte Differentiation of Human Pluripotent Stem Cells. Current protocols in human genetics. 2015;87:21.3.1–21.3.15.

30. Burridge PW, Matsa E, Shukla P, Lin ZC, Churko JM, Ebert AD, Lan F, Diecke S, Huber B, Mordwinkin NM, Plews JR, Abilez OJ, Cui B, Gold JD, Wu JC. Chemically defined generation of human cardiomyocytes. Nature methods. 2014;11:855–860. [PubMed: 24930130]
31. Gu Y, Gorelik J, Spohr HA, Shevchuk A, Lab MJ, Harding SE, Vodyanoy I, Klenerman D, Korchev YE. High-resolution scanning patch-clamp: new insights into cell function. FASEB J. 2002;16:748–50. [PubMed: 11923226]
32. Kim B, Matsuoka S. Cytoplasmic Na^+-dependent modulation of mitochondrial Ca^{2+} via electrogenic mitochondrial Na^+-Ca^{2+} exchange. J Physiol. 2008;586(6):1683–97. [PubMed: 18218682]
33. Sag CM, Wagner S, Maier LS. Role of oxidants on calcium and sodium movement in healthy and diseased cardiac myocytes. Free Radic Biol Med. 2013;63:338–49. [PubMed: 23732518]
34. Görlach A, Bertram K, Hudecova S, Krizanova O. Calcium and ROS: A mutual interplay. Redox Biol. 2015;6:260–271. [PubMed: 26296072]
35. Adhihetty PJ, Ljubicic V, Menzies KJ, Hood DA. Differential susceptibility of subsarcolemmal and intermyofibrillar mitochondria to apoptotic stimuli. Am J Physiol Cell Physiol. 2005;289(4):C994–C1001. [PubMed: 15901602]
36. Murphy E, Eisner DA. Regulation of intracellular and mitochondrial sodium in health and disease. Circ Res. 2009;104(3):292–303. [PubMed: 19213964]
37. Glancy B, Hartnell LM, Malide D, Yu ZX, Combs CA, Connelly PS, Subramaniam S, Balaban RS. Mitochondrial reticulum for cellular energy distribution in muscle. Nature. 2015;523:617–20. [PubMed: 26223627]
38. Glancy B, Hartnell LM, Combs CA, Fenmou A, Sun J, Murphy E, Subramaniam S, Balaban RS. Power Grid Protection of the Muscle Mitochondrial Reticulum. Cell reports. 2017;19:487–496. [PubMed: 28423313]
39. Miragoli M, Sanchez-Alonso JL, Bhargava A, Wright PT, Sikkel M, Schobesberger S, Diakonov I, Novak P, Castaldi A, Cattaneo P, Lyon AR, Lab MJ, Gorelik J. Microtubule-Dependent Mitochondria Alignment Regulates Calcium Release in Response to Nanomechanical Stimulus in Heart Myocytes. Cell Rep. 2016;14(1):140–151. [PubMed: 26725114]
40. Hong T and Shaw RM. Cardiac T-Tubule Microanatomy and Function. Physiological reviews. 2017;97:227–252. [PubMed: 27881552]
41. Lavorato M, Huang TQ, Iyer VR, Perni S, Meissner G and Franzini-Armstrong C. Dyad content is reduced in cardiac myocytes of mice with impaired calmodulin regulation of RyR2. J Muscle Res Cell Motil. 2015;36:205–14. [PubMed: 25694159]
42. Veeraraghavan R, Lin J, Hoeker GS, Keener JP, Gourdie RG, Poelzing S. Sodium channels in the Cx43 gap junction perinexus may constitute a cardiac ephapse: an experimental and modeling study. Pflugers Arch. 2015;467(10):2093–105. [PubMed: 25578859]
43. Luongo TS, Lambert JP, Gross P, Nwokedi M, Lombardi AA, Shanmughapriya S, Carpenter AC, Kolmetzky D, Gao E, van Berlo JH, Tsai EJ, Molkentin JD, Chen X, Madesh M, Houser SR, Elrod JW. The mitochondrial Na^+/Ca^{2+} exchanger is essential for Ca^{2+} homeostasis and viability. Nature. 2017;545(7652):93–97. [PubMed: 28445457]
44. Palty R, Silverman WF, Hershfinkel M, Caporale T, Sensi SL, Parnis J, Nolte C, Fishman D, Shoshan-Barmatz V, Herrmann S, Khananshvili D, Sekler I. NCLX is an essential component of mitochondrial Na^+/Ca^{2+} exchange. Proc Natl Acad Sci USA. 2010;107:436–441. [PubMed: 20018762]
45. Giorgi C, Marchi S, Pinton P. The machineries, regulation and cellular functions of mitochondrial calcium. Nat Rev Mol Cell Biol. 2018;19(11):713–730. [PubMed: 30143745]
46. Palty R, Ohana E, Hershfinkel M, Volokita M, Elgazar V, Beharier O, Silverman WF, Argaman M, Sekler I. Lithium-calcium exchange is mediated by a distinct potassium-independent sodium-calcium exchanger. J Biol Chem. 2004; 279(24):25234–40. [PubMed: 15060069]
47. Bernardi P, von Stockum S. The permeability transition pore as a Ca^{2+} release channel: new answers to an old question. Cell Calcium 2012; 52(1):22–7. [PubMed: 22513364]
48. Verkhratsky A, Trebak M, Perocchi F, Khananshvili D, Sekler I. Crosslink between calcium and sodium signalling. Exp Physiol. 2018;103(2):157–169. [PubMed: 29210126]

49. Despa S. Myocyte [Na^+]i Dysregulation in Heart Failure and Diabetic Cardiomyopathy. Front Physiol. 2018;9:1303. [PubMed: 30258369]
50. Skogestad J, Lines GT, Louch WE, Sejersted OM, Sjaastad I, Aronsen JM. Evidence for heterogeneous subsarcolemmal Na(+) levels in rat ventricular myocytes. Am J Physiol Heart Circ Physiol. 2019;316(5):H941–H957. [PubMed: 30657726]
51. Rizzuto R, De Stefani D, Raffaello A, Mammucari C. Mitochondria as sensors and regulators of calcium signalling. Nat Rev Mol Cell Biol. 2012;13(9):566–78. [PubMed: 22850819]
52. De La Fuente S, Lambert JP, Nichtova Z, Fernandez Sanz C, Elrod JW, Sheu SS, Csordás G. Spatial Separation of Mitochondrial Calcium Uptake and Extrusion for Energy-Efficient Mitochondrial Calcium Signaling in the Heart. Cell Rep. 2018;24(12):3099–3107. [PubMed: 30231993]
53. Sekler I, Hershfinkel M, Nita II. The mitochondrial Na^+/Ca^{2+} exchanger-NCLX is an integrating hub for glucose dependent Na^+ and Ca^{2+} signaling in pancreatic β cells. FASEB J. 2013;27:xxx.
54. Nita II, Hershfinkel M, Kantor C, Rutter GA, Lewis EC, Sekler I. Pancreatic β-cell Na^+ channels control global Ca^{2+} signaling and oxidative metabolism by inducing Na^+ and Ca^{2+} responses that are propagated into mitochondria. FASEB J. 2014;28:3301–3312. [PubMed: 24719357]
55. Kim MS and Usachev YM. Mitochondrial Ca^{2+} cycling facilitates activation of the transcription factor NFAT in sensory neurons. J Neurosci. 2009;29:12101–12114. [PubMed: 19793968]
56. Nita II, Caspi Y, Gudes S, Fishman D, Lev S, Hersfinkel M, Sekler I, Binshtok AM. Privileged crosstalk between TRPV1 channels and mitochondrial calcium shuttling machinery controls nociception. Biochim Biophys Acta. 2016;1863:2868–2880. [PubMed: 27627464]
57. Carrithers MD, Chatterjee G, Carrithers LM, Offoha R, Iheagwara U, Rahner C, Graham M, Waxman SG. Regulation of podosome formation in macrophages by a splice variant of the sodium channel SCN8A. J Biol Chem. 2009;284(12):8114–26. [PubMed: 19136557]
58. Kostic M and Sekler I. Function, regulation and physiological role of the mitochondrial Na^+/Ca^{2+} exchanger, NCLX. Current Opinion in Physiology. 2018;3:63–70.
59. Palty R, Hershfinkel M, Sekler I. Molecular identity and functional properties of the mitochondrial Na^+/Ca^{2+} exchanger. J Biol Chem. 2012;287(38):31650–7. [PubMed: 22822063]
60. Griffiths EJ. Mitochondrial calcium transport in the heart: physiological and pathological roles. J. Mol. Cell Cardiol 2009;46:789–803. [PubMed: 19285504]
61. Boyman L, Williams GS, Khananshvili D, Sekler I, Lederer WJ. NCLX: the mitochondrial sodium calcium exchanger. J. Mol. Cell Cardiol. 2013;59:205–213. [PubMed: 23538132]
62. Cox DA, Conforti L, Sperelakis N, Matlib MA. Selectivity of inhibition of Na(+)-Ca^{2+} exchange of heart mitochondria by benzothiazepine CGP-37157. J Cardiovasc Pharmacol. 1993;21:595–599. [PubMed: 7681905]
63. Maack C, Cortassa S, Aon M, Ganesan AN, Liu T, O'Rourke B. Elevated cytosolic Na^+ decreases mitochondrial Ca^{2+} uptake during excitation-contraction coupling and impairs energetic adaptation in cardiac myocytes. Circ. Res 2006;99:172–182. [PubMed: 16778127]
64. Samanta K, Mirams GR, Parekh AB. Sequential forward and reverse transport of the Na^+ Ca^{2+} exchanger generates Ca^{2+} oscillations within mitochondria. Nat Commun. 2018;9(1):156. [PubMed: 29323106]
65. Aon MA, Cortassa S, Marbán E, O'Rourke B. Synchronized whole cell oscillations in mitochondrial metabolism triggered by a local release of reactive oxygen species in cardiac myocytes. J Biol Chem. 2003;278(45):44735–44. [PubMed: 12930841]
66. Wang HJ, Li YL, Zhang LB, Zucker IH, Gao L, Zimmerman MC, Wang W. Endogenous reactive oxygen species modulates voltage-gated sodium channels in dorsal root ganglia of rats. J Appl Physiol. 1985;2011;110(5):1439–47. [PubMed: 21292836]
67. Liu M, Liu H, Dudley SC Jr. Reactive oxygen species originating from mitochondria regulate the cardiac sodium channel. Circ Res. 2010;107(8):967–74. [PubMed: 20724705]
68. Park DS, Fishman GI. SCN5A: the greatest HITS collection. J Clin Invest. 2018;128(3):913–915. [PubMed: 29457788]
69. Jiang D, Zhao L, Clapham DE. Genome-wide RNAi screen identifies Letm1 as a mitochondrial Ca^{2+}/H^+ antiporter. Science 2009;326(5949):144–7. [PubMed: 19797662]

70. Lu X, Kwong JQ, Molkentin JD, Bers DM. Individual cardiac mitochondria undergo rare transient permeability transition pore openings. Circ. Res 2016;118: 834–841. [PubMed: 26712344]

71. Gadicherla AK, Wang N, Bulic M, Agullo-Pascual E, Lissoni A, De Smet M, Delmar M, Bultynck G, Krysko DV, Camara A, Schlüter KD, Schulz R, Kwok WM7, Leybaert L. Mitochondrial Cx43 hemichannels contribute to mitochondrial calcium entry and cell death in the heart. Basic Res Cardiol. 2017;112(3):27. [PubMed: 28364353]

72. Boengler K, Stahlhofen S, van de Sand A, Gres P, Ruiz-Meana M, Garcia-Dorado D, Heusch G, Schulz R. Presence of connexin 43 in subsarcolemmal, but not in interfibrillar cardiomyocyte mitochondria. Basic Res Cardiol. 2009;104(2):141–7. [PubMed: 19242638]

73. Takahashi M, Hood DA. Protein import into subsarcolemmal and intermyofibrillar skeletal muscle mitochondria. Differential import regulation in distinct subcellular regions. J Biol Chem. 1996;271(44):27285–91. [PubMed: 8910303]

74. Holmuhamedov EL, Oberlin A, Short K, Terzic A, Jahangir A. Cardiac subsarcolemmal and interfibrillar mitochondria display distinct responsiveness to protection by diazoxide. PLoS One. 2012;7(9):e44667. [PubMed: 22973464]

75. Fekete A, Franklin L, Ikemoto T, Rózsa B, Lendvai B, Sylvester Vizi E, Zelles T. Mechanism of the persistent sodium current activator veratridine-evoked calcium elevation: implication for epilepsy. J. Neurochem 2009;111:745–756. [PubMed: 19719824]

76. Kovács R, Kardos J, Heinemann U, Kann O. Mitochondrial calcium ion and membrane potential transients follow the pattern of epileptiform discharges in hippocampal slice cultures. J. Neurosci 2005;25:4260–4269. [PubMed: 15858052]

77. Griffiths EJ. Reversal of mitochondrial sodium/calcium exchange during metabolic inhibition in rat cardiomyocytes. FEBS Lett. 1999;453:400–404. [PubMed: 10405185]

78. Bermudez-Hernandez K, Keegan S, Whelan DR, Reid DA, Zagelbaum J, Yin Y, Ma S, Rothenberg E, Fenyö D. A Method for Quantifying Molecular Interactions Using Stochastic Modelling and Super-Resolution Microscopy. Sci Rep. 2017;7(1):14882. [PubMed: 29093506]

79. Montnach J, Agullo-Pascual E, Tadros R, Bezzina CR, Delmar M. Bioinformatic analysis of a plakophilin-2-dependent transcription network: implications for the mechanisms of arrhythmogenic right ventricular cardiomyopathy in humans and in boxer dogs. Europace. 2018;20:iii125–iii132. [PubMed: 30476063]

NOVELTY AND SIGNIFICANCE

What Is Known?

- The voltage-gated sodium channels, formed by the protein $Na_v1.5$, carry the excitatory inward current (the sodium current) that is responsible for the action potential upstroke in adult cardiac ventricular myocytes.
- $Na_v1.5$ channels localize to different subdomains within the myocyte, associating with other molecules in a domain-specific manner.
- Mitochondrial function can alter the magnitude and properties of the sodium current.

What New Information Does This Article Contribute?

- $Na_v1.5$ clusters that localize to the membrane region between two z-lines (the "crest" of the sarcomere) are in close apposition to subsarcolemmal mitochondria and to the mitochondrial Na^+/Ca^{2+} exchanger.
- This anatomical proximity leads to a functional relation between $Na_v1.5$ and the mitochondrial Na^+/Ca^{2+} exchanger.
- $Na_v1.5$ channel malfunction leads to unbalanced mitochondrial calcium dynamics, potentially impacting cell metabolism.

Na-channels form macromolecular complexes that, in adult ventricular myocytes, cluster at specific subdomains. Dysfunction of the channel itself, or of its partners, can lead to arrhythmias that cause sudden cardiac death. The relation between Na-channels and mitochondrial function has been described in one direction only: mitochondrial byproducts (such as ROS) affect sodium current. Here we show that this relation is reciprocal, namely, Na-channel activity influences mitochondrial function. Using imaging techniques, we describe the deterministic localization of Na-channels and subsarcolemmal mitochondria, where we primarily locate the mitochondrial Na^+/Ca^{2+} exchanger. Functionally, the blockade of Na-channels leads to a local mitochondrial Ca^{2+} accumulation and ROS production. We propose that NCLX is powered by the entry of Na^+ through Na-channels to properly extrude Ca^{2+}. This proposed model for electro-metabolic coupling redefines $Na_v1.5$ as a key regulator of cell metabolism and opens a new window to understand electrical and structural disorders of the heart.

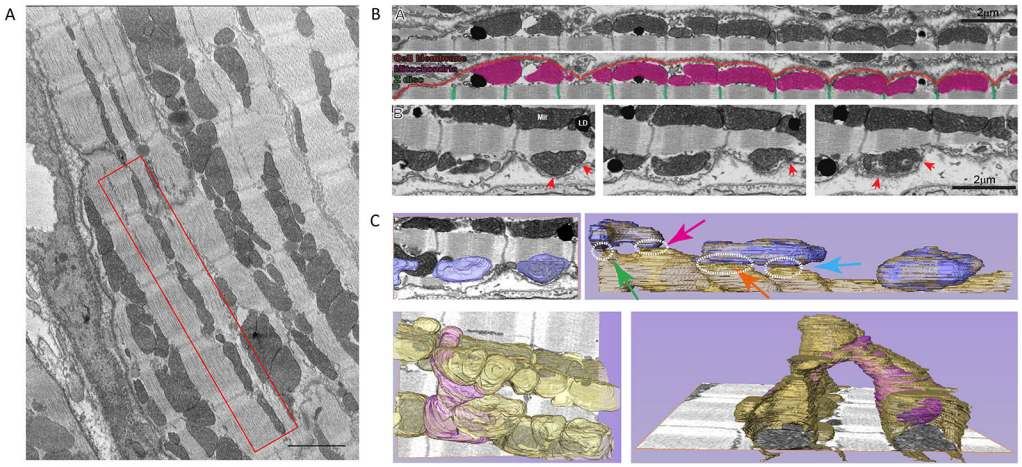

Figure 1. Mitochondria in close apposition to sarcolemma.

A. Focused Ion Beam-Scanning Electron Microscopy (FIB-SEM) image of ventricular myocytes. Notice the presence of mitochondria between z-disks (red box). Scale bar 2 μm. **B**. FIB-SEM single plane of complete 3D-volumetric image of cell membrane and subjacent mitochondria. Notice mitochondria under the crest. Enlarged images in bottom frames: sequential z-sections showing proximity of membranes and points where membranes come in close apposition (red arrows). **C**. Segmentation analysis of subsarcolemmal mitochondria connecting to mitochondrial reticulum. Top left: Mitochondria in bottom images of panel B, highlighted in blue. Top right: Segmentation of layers below shows subsarcolemmal mitochondria coupling to first chain of interfibrillar mitochondria. Dotted circles identify points of proximity. Lower panel in left shows subsarcolemmal mitochondria (purple) that bifurcates to reach two interfibrillar chains. Bottom right: bifurcating mitochondrial from a different angle. Through these connections, mitochondria form a complete reticulum, as documented by Glancy et al.[37,38]

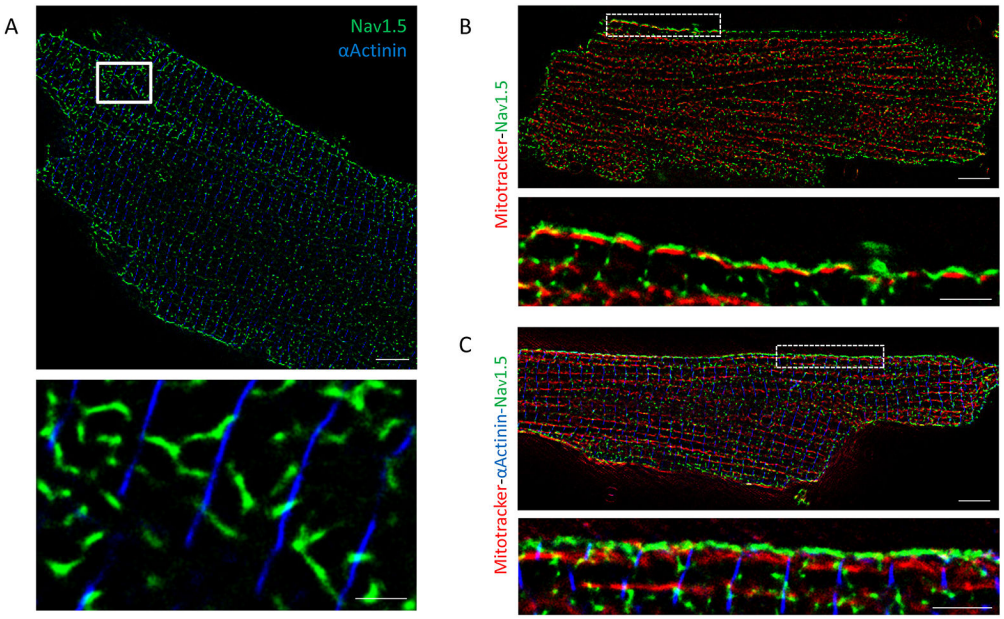

Figure 2. $Na_v1.5$ is found between z-disks close to mitochondria.

A. Stochastic optical reconstruction microscopy (STORM) image of adult ventricular myocyte. Blue: α-actinin as marker of z-disk. Green: $Na_v1.5$. White-boxed area enlarged in bottom panel. Scale bars 5 μm. Inset scale bar 1 μm. Apparent misalignment of α-actinin lines is due to cell surface curvature. Notice that large clusters of $Na_v1.5$ fall not on α-actinin (the expectation for costameric localization), but in-between, corresponding to the crest. **B-C**. STORM-acquired images of Mitotracker (red), $Na_v1.5$ (green) and α-Actinin (only in panel C, blue) in single myocytes dissociated from wild-type mice. White-boxed areas enlarged in respective bottom panels. Scale bars 5 μm. Inset scale bar 2 μm. Notice alignment of $Na_v1.5$ with SSM at cell surface, spaced by marker of z-disk.

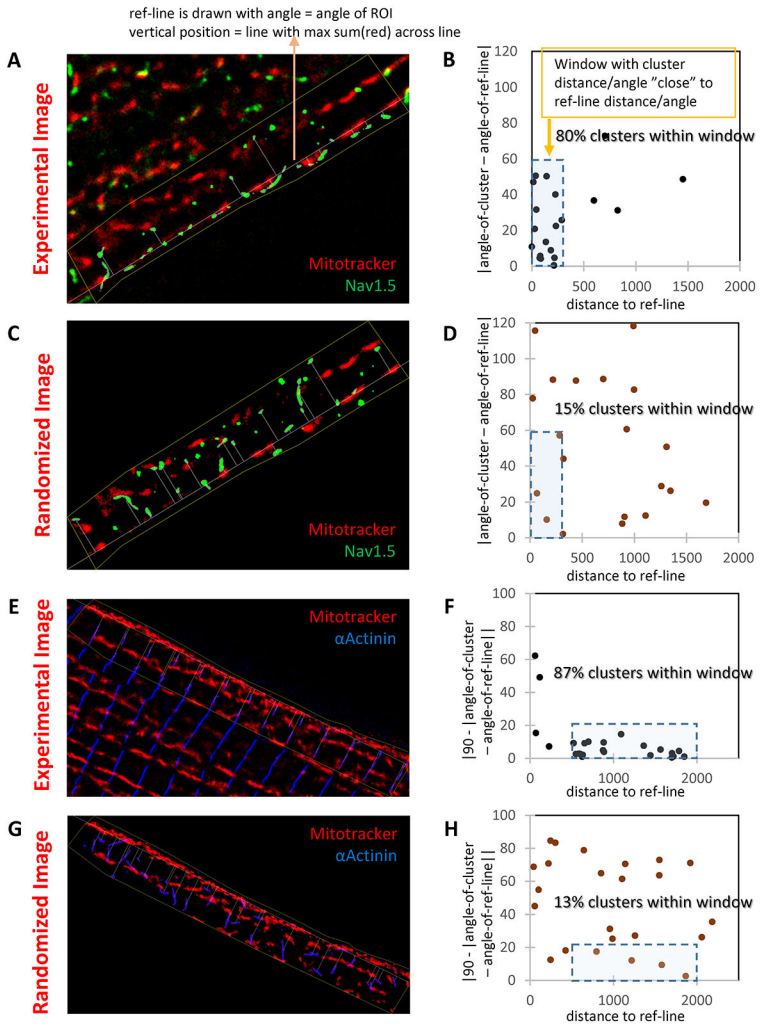

Figure 3. $Na_V1.5$ localizes on top of SSM in a deterministic matter.

A-B: STORM-acquired image of Mitotracker (red) and $Na_V1.5$ (green) from the lateral membrane of an adult murine myocyte ("Experimental image"; **A**) and data analysis (**B**). Reference line was traced over the first string of mitochondria under the cell membrane (SSM). This line was used as reference to measure distance to centroid of the $Na_V1.5$ cluster (abscisae in B) and its inclination, namely, the angle of the long axis of the ellipse defining the cluster (ordinates in B). A window of 300 nm and up to 60° in inclination captured 80% of the clusters. Distribution was compared to that obtained by modeling a random distribution of green clusters over the same region of interest (**C**; "randomized image"). In that condition, only 15% of clusters fell within the same window (**D**). To validate the model, results were compared to those obtained for a domain established by clusters of known architecture, namely, α-actinin (**E**: "Experimental image" of Mitotracker (red) and α-Actinin (blue). Analysis in **F**. In this case, to enhance visualization, the angle of inclination is reported as 90-angle (so perpendicular lines cluster around zero). A similar experiment in the "randomized image" is presented in **G-H**. As predicted, α-actinin is tightly organized in relation to mitochondria, and such organization is lost when clusters distribute randomly.

Distance to reference line measured in nm. Similar results were obtained in n=28 cells from N=4 mice.

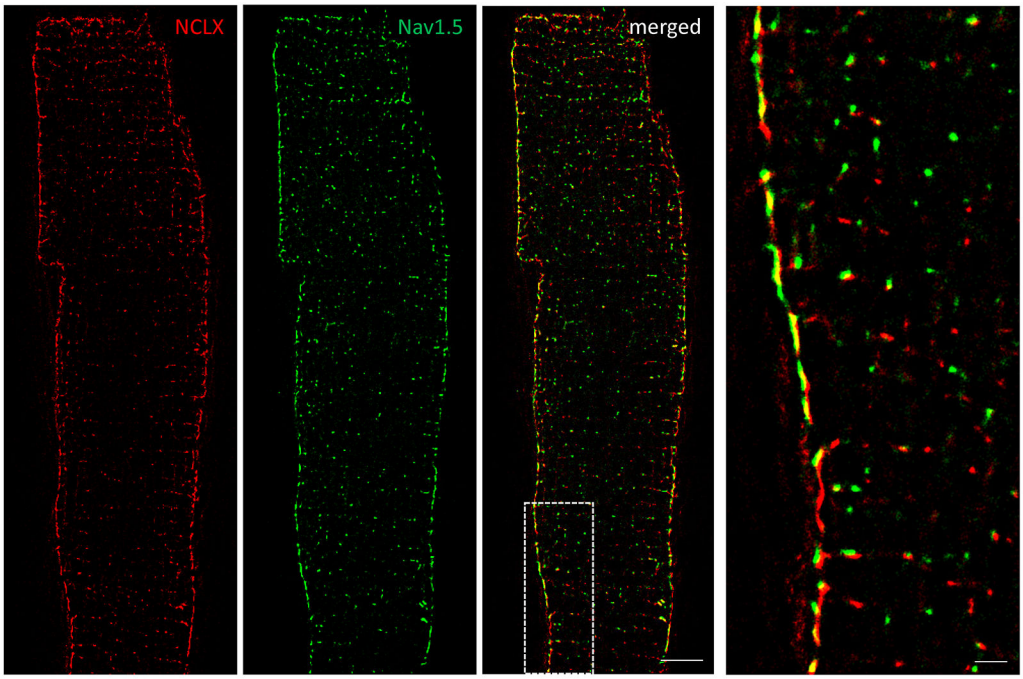

Figure 4. Mitochondrial NCLX is mainly found in SSM near $Na_V1.5$ clusters.

Dual-color stochastic optical reconstruction microscopy (STORM)-acquired images of NCLX (red) and $Na_V1.5$ (green) in single myocytes dissociated from wild-type mice. White-boxed area enlarged in right image. Notice abundance of NCLX signal at lateral membrane and proximity to $Na_V1.5$ clusters. Scale bar 5 μm. Inset scale bar 1 μm.

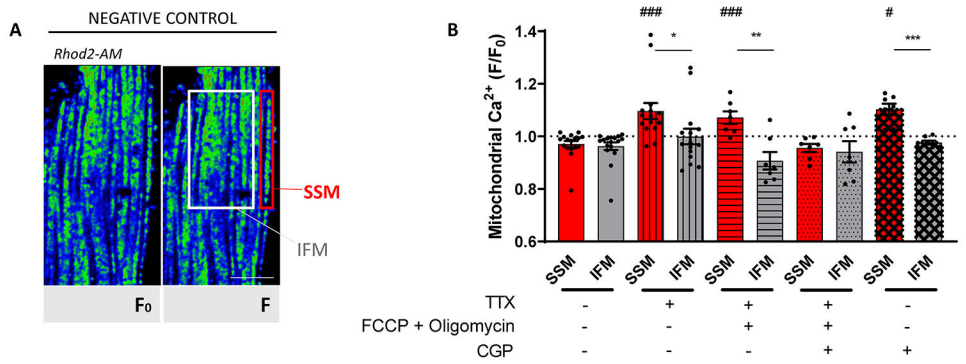

Figure 5. Mitochondrial Ca^{2+} in relation to sodium channel activity.

A. Confocal 2D images of cardiomyocytes loaded with Rhod 2-AM at 4°C and then incubated at 37°C for 3-5 hours (see Methods). Two regions were defined, SSM (first string of mitochondria immediately below cell surface) and IFM (in the interior of the cell). **B**. Quantitative analysis of F/F_0 (F corresponds to Rhod2-AM intensity at rest, and F_0 to Rhod2-AM intensity after treatment) ratio under conditions described in the table below. Notice increased fluorescence emission units (mitochondria) after tetrodotoxin (TTX), TTX +FCCP+Oligomycin and CGP-37157 treatment, particularly in SSM. The ratio F/F_0 of Rhod-2 fluorescence intensities was compared between SSM and IFM: higher ratio reflects more mitochondrial Ca^{2+} accumulation. Scale bar 10 μm. +TTX: 15 cells from 8 mice; +TTX+FCCP+Oligomycin: 7 cells from 4 mice; +TTX+FCCP+Oligomycin+CGP-37157: 7 cells from 3 mice; CGP-37157: 6 cells from 3 mice; Negative control: 17 cells from 5 mice. Student's t-test: between SSM and IFM for each treatment: *p<0.05 *vs* SSM, **p<0.01 *vs* SSM, ***p<0.001 *vs* SSM; between treatment *vs* negative control: #p<0.05 *vs* negative control, ###p<0.001 *vs* negative control.

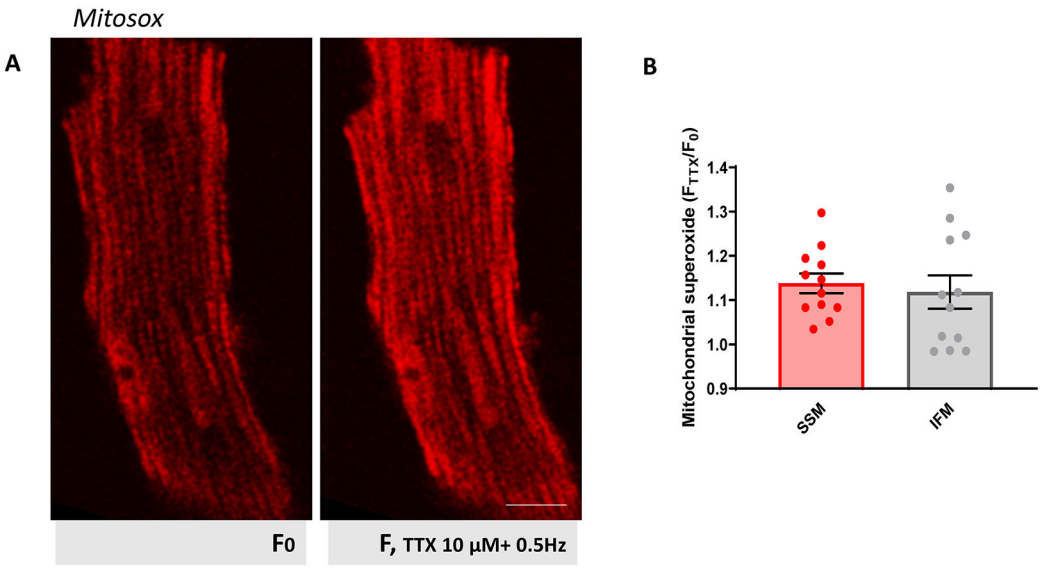

Figure 6. Increased superoxide production after TTX.

A. Confocal 2D images of cardiomyocytes loaded with MitoSOX (see Methods). Two images from same cell are shown: at rest (F_0; left), and after 10 µmol/L addition of TTX (F; right). Notice brighter fluorescence at SSM at resting conditions compared to IFM. Scale bar 10 µm. **B**. Ratio F_{TTX}/F_0 of MitoSOX fluorescence intensities was compared between SSM and IFM: higher ratio reflects more ROS produced. Average was then plotted. N=3 mice, n=12 cells. No statistical differences (Student's t-test).

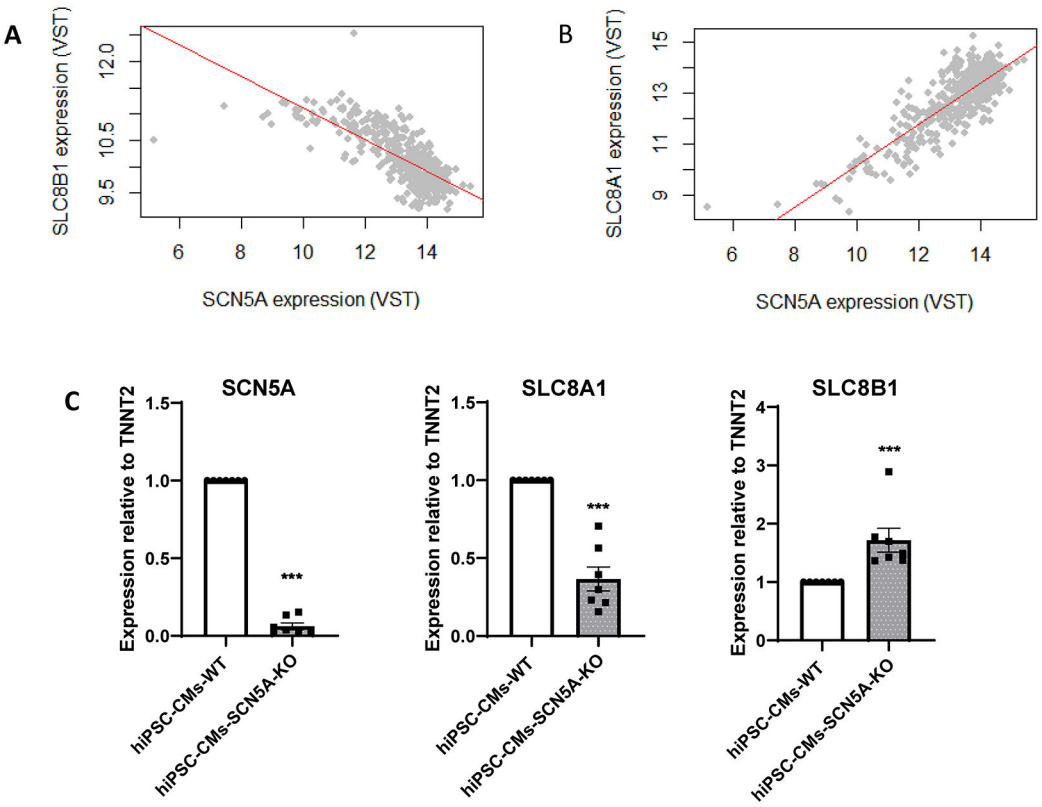

Figure 7. *SLC8B1* (encoding NCLX), negatively correlates with *SCN5A*.

A-B. Association analysis of human left ventricle transcriptome in relation to *SCN5A* expression: correlation between expression of *SLC8B1* (panel A) or *SLC8A1* (panel B) *vs* *SCN5A* expression. Each point represents the normalized level (VST, variance stabilizing transformation) of *SCN5A* *vs* that of *SLC8B1* (A) or *SLC8A1* (B) for one individual in the dataset. Notice the positive slope (=positive correlation) between *SCN5A* and *SLC8A1* (plasma membrane NCX) and negative correlation with *SLC8B1* (mitochondrial NCLX), suggesting that *SCN5A* transcript levels correlate with expression of both in human heart. **C**. qPCR for *SCN5A*, *SLC8A1* and *SLC8B1* in hiPSC-CMs wild-type (WT) and SCN5A-KO. Notice drastic reduction in *SCN5A* and increase in *SLC8B1* in hiPSC-CM SCN5A-KO. N=7. Statistical test: Mann Whitney U-test between SCN5A-KO and WT for each gene. ***$p<0.001$ *vs* WT.